Heat Transfer Performance analysis of a P-Type ribbed Solar Air Heater (P-SAH)

Sachindra Kumar Rout[1], Sanjib Kumar Rout[1] and Suvaranjan Sutar[1]

[1] C V RAMAN GLOBAL UNIVERSITY, BHUBANESWAR, INDIA-752054, City (INDIA)

Abstract

Solar energy offers an effective and sustainable means for a variety of practical uses, including food drying, crop processing, space heating, and air circulation. These processes can be efficiently performed with the help of a Solar Air Heater (SAH). In this work, a comprehensive numerical investigation is carried out on an SAH featuring P-shaped ribs placed on the absorber plate in different transverse arrangements with respect to the airflow. Each rib configuration is examined separately. The simulations are executed using ANSYS Fluent to solve the fundamental conservation equations of mass, momentum, and energy. A constant heat flux of 1000 W/m² is applied on the absorber surface. Major influencing factors such as inlet air velocity and rib dimensions (height and pitch) are studied for Reynolds numbers between 3,400 and 20,000, with rib pitches varying from 6.26 to 18.75. The influence of rib geometry on pressure losses is also explored. Flow characteristics are illustrated through contour plots of temperature, pressure, and velocity, providing a clear understanding of the system's behavior. The findings indicate a considerable improvement in thermal performance, with the best results achieved at a rib pitch of 15.62, corresponding to a Thermal Enhancement Ratio (TER) of 2.35.

Keywords: CFD study , Solar air heater, SST k-ε model, turbulent heat transfer, fluid flow

1. Introduction

In the last few decades, the rapid expansion of industries and technological progress has sharply increased global energy needs, leading to a strong shift toward renewable and eco-friendly energy options. Among these, solar energy stands out as a dependable and sustainable choice because it is abundant, easily available, and environmentally safe. Unlike traditional fossil fuels such as coal, petroleum, or natural gas, the generation of solar power does not release harmful greenhouse gases, nor does it contribute to air or water contamination. This makes it a key factor in achieving long-term ecological stability.

Flat-plate solar collectors are widely used components in solar air heater (SAH) systems, particularly suited for low- and medium-temperature operations such as space heating, crop and food drying, and water heating. These systems harness solar radiation effectively, cutting down on dependence on nonrenewable energy sources while reducing operating expenses and carbon emissions. As depicted in Figure 1, SAHs have found diverse applications in agricultural drying, building space heating, and marine-related processes where moderate thermal energy is sufficient.

However, the performance of traditional SAHs is often limited by poor convective heat transfer between the absorber surface and the air stream, resulting in low overall thermal efficiency. To overcome this drawback, researchers have developed surface modification techniques by introducing artificial roughness on the absorber plate. This roughness promotes turbulence close to the wall, disturbs the laminar sub layer, and enhances the rate of heat transfer without causing excessive pressure loss in the system.

Computational Fluid Dynamics (CFD) has evolved into an essential technique for analyzing modified solar air heating systems. It enables precise examination of airflow behavior, temperature variation, and pressure losses within the duct. While experimental research has confirmed the benefits of using roughened absorber plates, numerical studies using CFD are

10.18086/swc.2025.02.16 Available at http://proceedings.ises.org

still comparatively fewer. Nevertheless, such analyses provide deep understanding and serve as a valuable approach for improving the thermo-hydraulic efficiency of solar air heaters.

This research examines the thermo-hydraulic behavior of a solar air heater[1] equipped with absorber plates containing P-shaped rib structures. The analysis is performed through CFD simulations carried out in ANSYS software. The study primarily explores how variations in rib thickness influence both thermal performance—quantified by the Nusselt number—and hydraulic behavior, indicated by the friction factor. The outcomes of this investigation aim to contribute to the design improvement and performance optimization of solar air heater systems for more effective heat transfer and energy utilization. Chaube et al.[2]conducted two-dimensional CFD investigation on SAH incorporating absorber plates with artificial surface roughness. The work explored ten distinct rib shapes—including rectangular, square, chamfered, and triangular profiles—to understand their influence on heat transfer and airflow behavior. Simulations were executed using FLUENT 6.1, with the SST k–ω turbulence model applied to accurately represent turbulent flow conditions. Among the various configurations analyzed, rectangular ribs measuring 3 × 5 mm demonstrated the best thermo-hydraulic efficiency. The computed data showed strong agreement with previously published experimental observations, validating the reliability of the numerical modeling technique. Sahu and Bhagoria[3] study investigated the effect of using transverse cracked ribs and reported that, for a pitch value of 20 under the specified flow conditions, the thermal efficiency improved by approximately 83.5%.Gupta et al.[4] research explored heat transfer improvement within a square duct equipped with three rib geometries—namely 90° straight, 90° saw-tooth, and 60° inclined cracked ribs. Of these configurations, the 60° inclined ribs delivered the highest enhancement in thermal performance. Nidhul et al.[5] examined a triangular-duct solar air heater equipped with rectangular ribs and revealed that a rib aspect ratio of 4 resulted in more than a 40% reduction in both exergy loss and environmental impact.Yadav and Bhagoria[6] used CFD with circular ribs on a SAH absorber, finding maximum Nusselt and friction factor ratios of 2.31 and 3.14, respectively. Karmare and Tikekar[7] evaluated the performance of a solar air heater (SAH) using ribs with square, triangular, and circular cross-sections. Numerous researchers have similarly investigated diverse rib geometries to improve SAH efficiency. Kumar and Layek[8] experimentally studied a rectangular SAH with staggered V-shaped ribs, achieving an optimal thermo-hydraulic performance index of 2.69 at P/e = 9, d/e = 4, and S/e = 6.15.

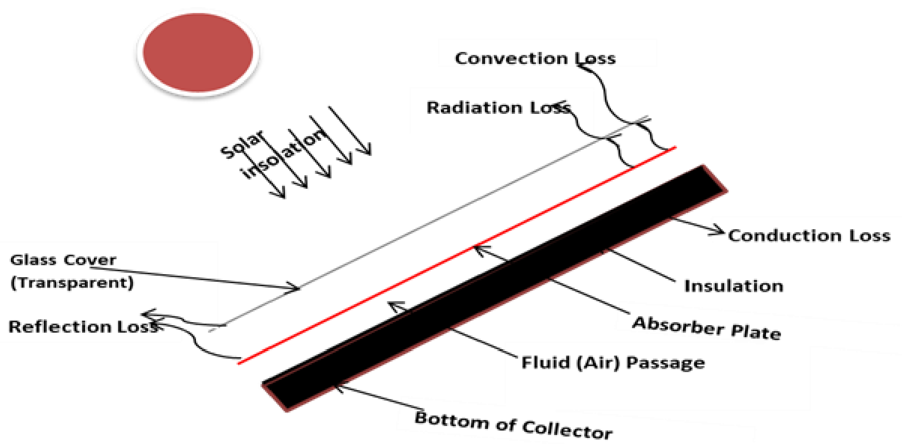

Figure 1. Solar air cheater schematic

2. Problem explanation

The system's behavior was primarily influenced by inlet air velocity and rib parameters[9] such as size, shape, and orientation. A 2D CFD model of the roughened SAH was developed, and Figure-2 presents the schematic of the computational setup used for simulation.

As illustrated in Figure 3, this study examines a P-type arrangement of transverse ribs to evaluate their influence on the thermo-hydraulic performance[10] of a roughened SAH. To simplify the CFD model, the following assumptions were applied:
i. The airflow in the computational region is modeled as two-dimensional, steady, and fully developed under turbulent conditions.

ii. A no-slip boundary condition is applied along all interfaces where the solid surfaces meet the fluid.

iii. The numerical discretization is performed exclusively for the fluid region of the model.

iv. Since variations in temperature and pressure are relatively small, the thermo physical properties of air, the absorber plate, and the insulated walls are assumed constant and evaluated at 300 K.

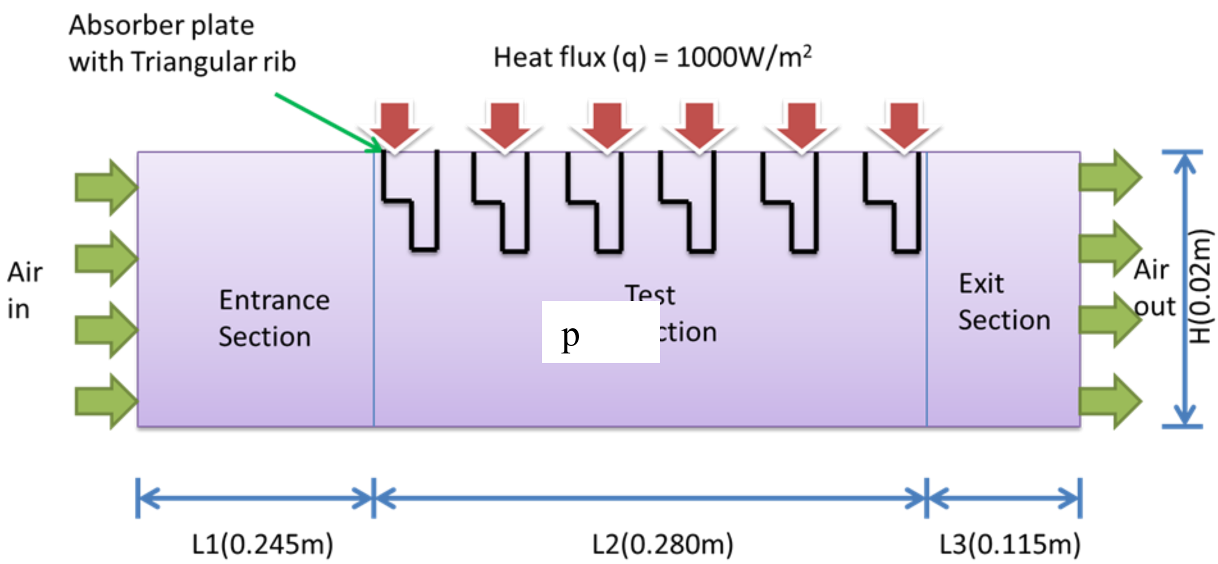

Figure.2 Computational area for P-Type ribbed SAH

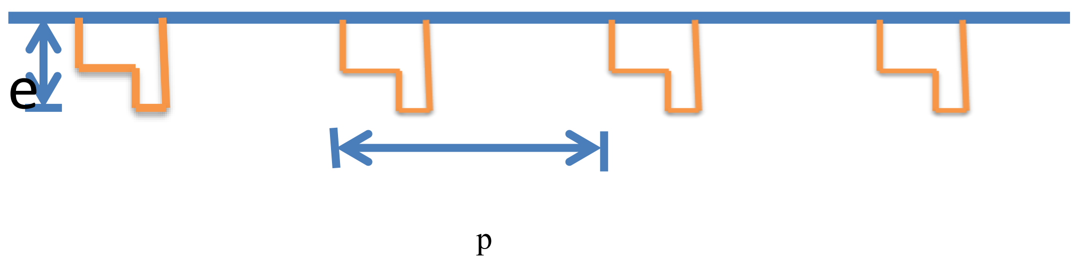

Figure.3 representation of ribs arranged in absorber plate

2.1 Geometry Details

Constructed as a rectangular duct, the SAH includes inlet, test, and outlet portions. According to ASHRAE specifications, the inlet length must be at least 5√(W×H) and the outlet length 2.5√(W×H). Table 1 presents the geometric parameters considered in this study.

Table 1. Different geometric and operating parameters

PARAMETER	PARAMETRIC VALUE
Inlet duct length	245mm
Test duct length	280mm
Exit duct length	115mm
Width of duct(W)	100mm
Height of duct(e)	20mm
Effective hydraulic diameter (h_D)	33.33mm
Roughness height ratio (e/h_D)	0.027
Roughness pitch ratio (p/e)	6.26,9.3,12.33,15.66,18.75
Heat flux	1000W/m^2
Reynolds number	3400,7000,13000,18000,20000

2.2 Analytical correlations employed in the study

Dittus-Boeltercorelation[11]	$\overline{Nu_s} = 0.023Re^{0.8}Pr^{0.4}$	
Blasius correlation[12]	$\overline{f_s} = 0.0791Re^{-0.25}$	
The quantity of heat mined from the absorber plate	$Q = hA_p(T_p - T_b)$	A_p= Effective area of the absorber surface T_p= Fluent-based estimation of absorber plate temperature T_b= Fluent-based evaluation of bulk mean temperature
Nusselt number for the SAH	$\overline{Nu_x} = hh_D/k$	
Hydraulic diameter of the duct	$D_h = \frac{4 \times A_f}{P_w}$	
The average friction factor	$\overline{f_r} = \frac{\{\Delta p \vert l\}}{2\rho v^2} h_D$	
Thermal enhancement ratio[13]	$TER = \frac{\left(\frac{Nu_r}{Nu_s}\right)}{\left(\frac{fr}{fs}\right)^{1/3}}$	

2.3 Governing equations

Mass balance

$$\frac{\partial(\rho u_i)}{\partial x_i} = 0 \quad (1)$$

Momentum balance

$$\frac{\partial(\rho u_i u_j)}{\partial x_i} = -\frac{\partial p}{\partial x_i} + \frac{\partial}{\partial x_j}\left[\mu\left(\frac{\partial u_i}{\partial x_j} + \frac{\partial u_j}{\partial x_i}\right)\right] + \frac{\partial}{\partial x_j}\left(-\rho\overline{u_i' u_j'}\right) \quad (2)$$

Energy balance

$$\frac{\partial(\rho u_i T)}{\partial x_i} = \frac{\partial}{\partial x_j}\left((\Gamma + \Gamma_t)\frac{\partial T}{\partial x_j}\right) \quad (3)$$

Where Γ *and* Γ_i are represented as

$$\Gamma = \frac{\mu}{P_r} \quad , \quad \Gamma_t = \frac{\mu}{P_{r_i}}$$

The differential equation for the renormalization group (RNG) model is as follows

$$\frac{\partial(\rho k u_i)}{\partial x_i} = \frac{\partial}{\partial x_j}\left(\alpha_k \mu_{eff}\frac{\partial k}{\partial x_j}\right) + G_k - \rho\varepsilon$$

$$\frac{\partial(\rho\varepsilon u_i)}{\partial x_i} = \frac{\partial}{\partial x_j}\left(\alpha_\varepsilon \mu_{eff}\frac{\partial \epsilon}{\partial x_j}\right) + C_{1e}\frac{\varepsilon}{k}(G_k) - C_{2\varepsilon}\rho\frac{\epsilon^2}{k} - R_\epsilon$$

α_k *and* α_ε represent inverse turbulent Prandtl numbers, which are important parameters for predicting turbulent flow behavior in the model. $\mu_{eff} = \mu + \mu_t$

$$\mu_t = \rho C_\mu \frac{k^2}{\varepsilon}$$

$$G_k = -\rho\mu_i'\mu_j'\frac{\partial u_j}{\partial x_i}$$

3. Numerical scheme

The governing equations were computed in ANSYS FLUENT using a pressure-based solver in combination with the SIMPLE scheme to couple pressure and velocity. The convergence criterion for residuals was fixed at 10^{-6}, with second-order upwind discretization applied to the pressure term and first-order upwind schemes used for the remaining variables.

Choosing a suitable turbulence model plays a key role in ensuring the accuracy of numerical simulations. Figure 4 illustrates the variation of the Nusselt number with Reynolds number for several models, namely the standard k–ε, RNG k–ε, RNG-standard, and SST k–ε formulations. Based on previous investigations, the RNG k–ε model combined with enhanced wall treatment has been shown to provide results that closely align.

4. Result discussion

This section presents an analysis of the heat transfer and fluid flow behavior of a solar air heater equipped with P-type ribs, along with a detailed discussion of the computational findings.

4.1 Impact of Reynolds number change on Nu and Fr.

Figure 5(a) illustrates the variation of the average Nusselt number with Reynolds number for different P/e ratios. A uniform velocity and constant flow rate are specified at the duct inlet. The ribs induce boundary layer separation and reattachment, forming vortices near rib edges and in the gaps between them. These vortices create localized turbulence, enhancing fluid mixing. Increasing the number of ribs intensifies flow obstruction, promotes boundary layer development, and elevates turbulence, which collectively improves heat transfer. Figure 5(b) illustrates how the average friction factor changes with Reynolds number for different P/e ratios at a relative roughness height of e/Dh = 0.048. The data indicate a declining trend in the friction factor as the Reynolds number increases. This behavior occurs because, with rising flow velocity, the boundary layer becomes thinner and the viscous sub layer experiences greater disturbance, which leads to a reduction in the overall friction factor.

with experimental observations. Hence, this model is adopted for the present analysis..

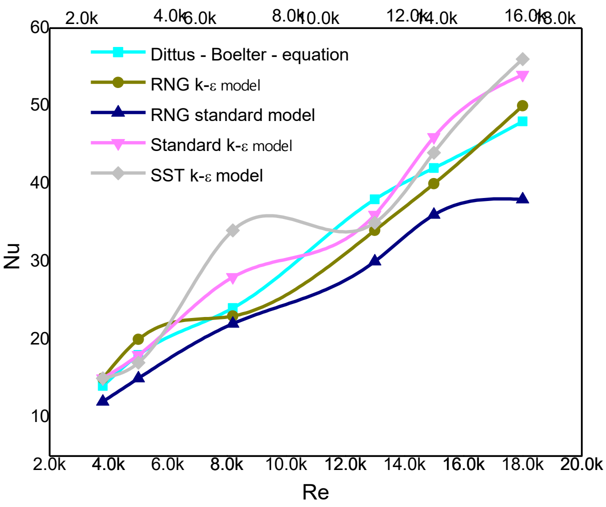

Fig.4.The Nusselt number versus Reynolds number plot for different turbulence models.

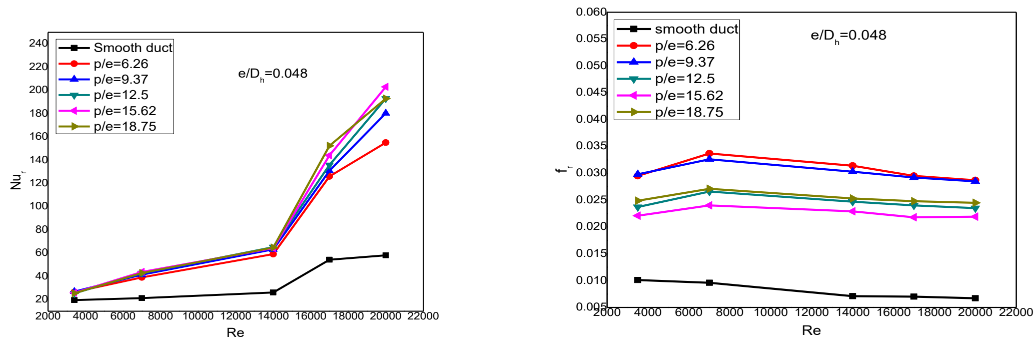

(a) (b)

Fig.5.(a) Graph between average Nu and Re (b) Graph between average Fr and Re.

4.2 Examination of turbulence behavior inside the SAH.

Figures 6 and 7 show the turbulent kinetic energy (TKE) and turbulence intensity in the SAH with a collector plate at p/e=15.62 and e/D_h=0.048 for Reynolds numbers of 3,400 and 20,000. The contour plots indicate that turbulence is highest between the first and second ribs and gradually decreases in downstream inter-rib regions. Maximum turbulence occurs near rib surfaces due to elevated shear stress, while eddies generated by air–rib interactions enhance both TKE and turbulence intensity. At higher Reynolds numbers, increased turbulence promotes stronger mixing, thereby improving heat transfer from the absorber plate.

4.3 **Thermo hydraulic performance analysis**

Figure 8 shows the variation of the thermal enhancement factor (TER) with Reynolds number for different p/e ratios in the solar air heater. At a given Reynolds number, TER increases with p/e up to an optimal value before declining. The maximum TER of 2.35 is achieved at Re=20,000. Additionally, decreasing the number of ribs reduces TER, with the greatest enhancement observed at p/e=15.62.

(a)

(b)

(C
)

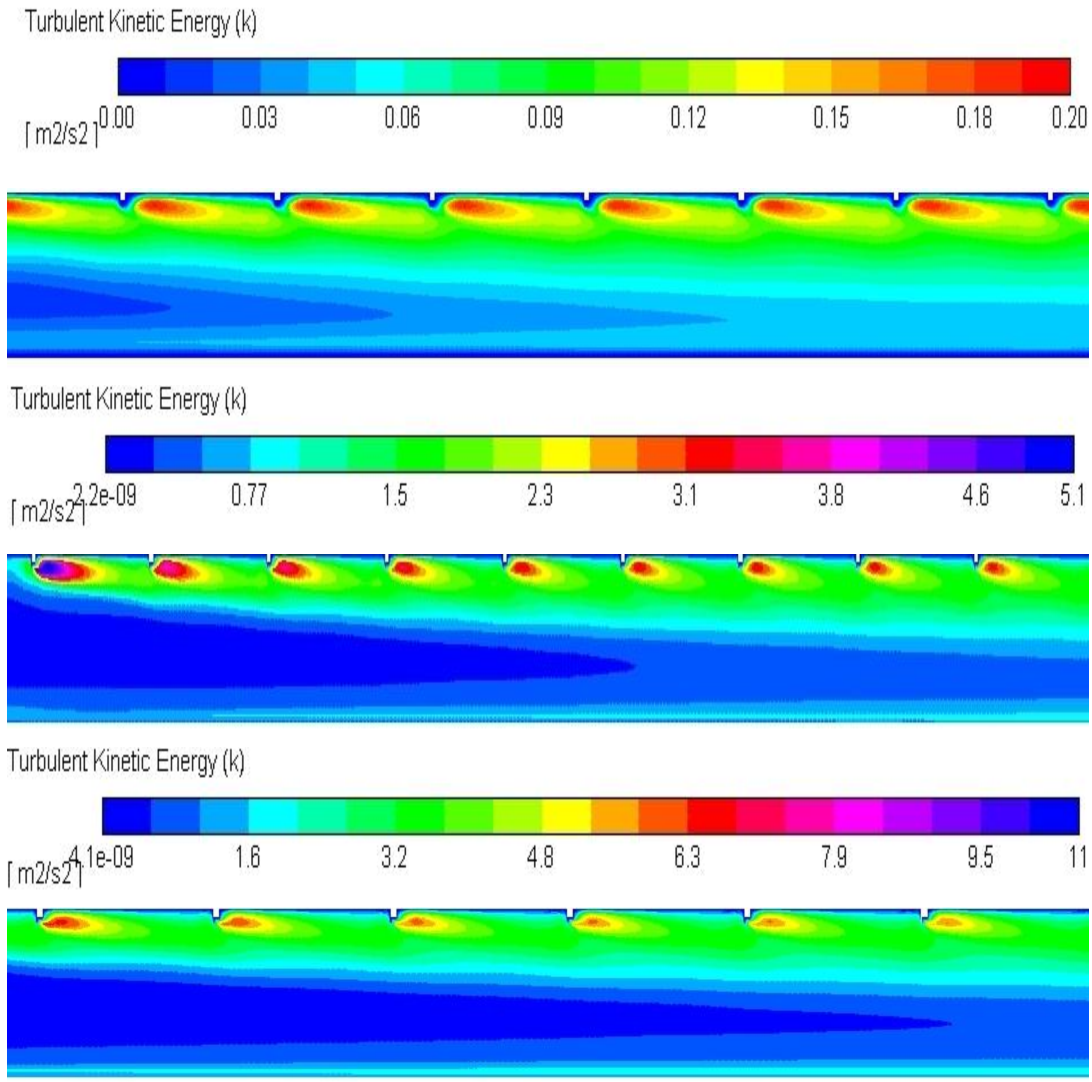

Fig.6 TKE contours for p/e=15.62 for Reynolds numbers of (a) 3400, (b) 18000 and (c) 20000

(a)

(b)

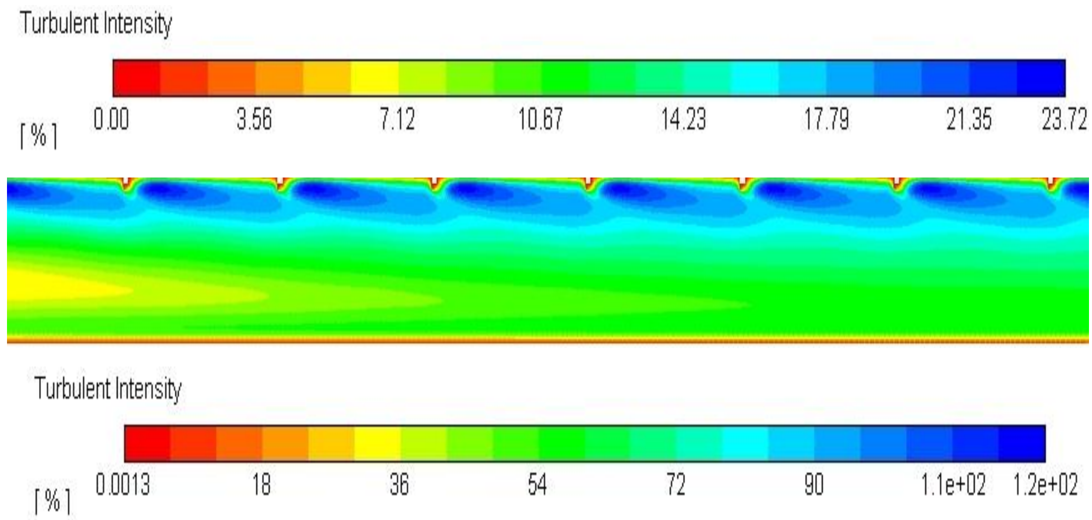

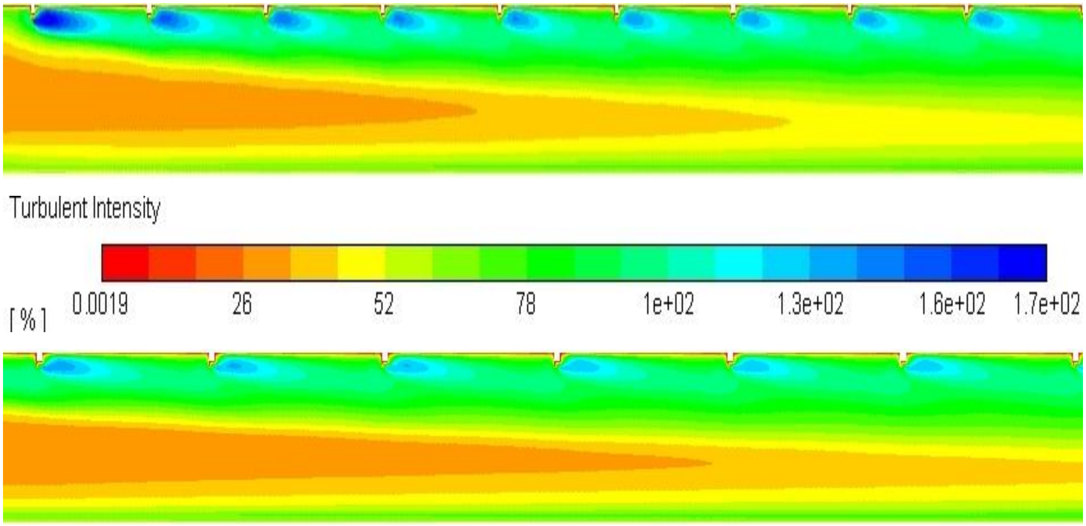

(c)

Figure 7: Contours for p/e=15.62 for Reynolds numbers of (a) 3400, (b) 18000 and (c) 20000

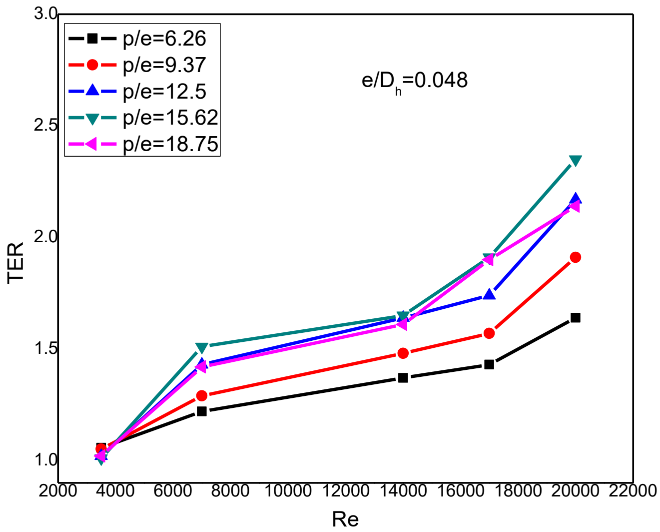

Figure. 8 Plot of TER for Different p/e at e/Dh=0.048

5. Conclusion

- A two-dimensional computational study was performed on a solar air heater fitted with P-shaped ribs on the absorber plate. In this investigation, the rib height was kept fixed, while the rib pitch was systematically varied over a broad range of Reynolds numbers to examine its effect on the Nusselt number (Nu) and friction factor (f). The addition of ribs significantly improved heat transfer performance, and the principal findings from the analysis are outlined below.
- The Reynolds number has a strong impact on both the Nusselt number and the friction factor. As the Reynolds number increases, the Nusselt number shows a rising trend, whereas the friction factor gradually declines.
- The highest Nusselt number is achieved for the P-type rib configuration with a relative pitch ratio of 15.62 at a Reynolds number of 20,000.
- At a Re of 7000, the f_r enhancement ratio spreads its peak, approximately at 4.4225, with a p/e of 6.26.

- At a relative pitch ratio (p/e) of 15.62 and a relative roughness height (e/Dh) of 0.048, the maximum thermal enhancement ratio (TER) is recorded at a Reynolds number of 20,000, attaining a value of 2.35.
- Graphical representations of temperature distribution and turbulence patterns for the P-type rib configuration provide a clear understanding of the flow dynamics and corresponding heat transfer behavior.

Acknowledgments

The authors gratefully acknowledge C. V. Raman Global University for the financial support provided for this research.

References

Sutar, S., et al., Numerical Investigation of Solar Air Heater for Space Heating Application. Applied Solar Energy, 2024. 60(5): p. 708-726.

Chaube, A., P. Sahoo, and S. Solanki, Analysis of heat transfer augmentation and flow characteristics due to rib roughness over absorber plate of a solar air heater. Renewable Energy, 2006. 31(3): p. 317-331.

Sahu, M. and J. Bhagoria, Augmentation of heat transfer coefficient by using 90 broken transverse ribs on absorber plate of solar air heater. Renewable energy, 2005. 30(13): p. 2057-2073.

Gupta, A., et al., Local heat transfer distribution in a square channel with 90 continuous, 90 saw tooth profiled and 60 broken ribs. Experimental Thermal and Fluid Science, 2008. 32(4): p. 997-1010.

Nidhul, K., et al., Influence of rectangular ribs on exergetic performance in a triangular duct solar air heater. Journal of Thermal Science and Engineering Applications, 2020. 12(5): p. 051010.

Yadav, A.S. and J. Bhagoria, Modeling and Simulation of Turbulent Flows through a Solar Air Heater Having Square-Sectioned Transverse Rib Roughness on the Absorber Plate. The Scientific World Journal, 2013. 2013(1): p. 827131.

Karmare, S. and A. Tikekar, Analysis of fluid flow and heat transfer in a rib grit roughened surface solar air heater using CFD. Solar Energy, 2010. 84(3): p. 409-417.

Kumar, D. and A. Layek, Experimental assessment of thermohydraulic performance of a rectangular solar air heater duct using twisted V-shaped staggered ribs. Journal of Thermal Science and Engineering Applications, 2023. 15(4): p. 041009.

Sutar, S., et al., Influence of Artificial Ribbing on the Thermal Performance of Solar Air Heaters: A Parametric Investigation. International Journal of Heat & Technology, 2025. 43(3).

Sutar, S., et al., Numerical investigation on the thermohydraulic performance of a solar air heater duct featuring parabolic rib turbulators on the absorber plate. Case Studies in Thermal Engineering, 2024. 64: p. 105399.

McAdams, W.H. and W.H. McAdams, Heat transmission. Vol. 3. 1954: McGraw-hill New York.

Blasius, H., Das aehnlichkeitsgesetz bei reibungsvorgängen in flüssigkeiten, in Mitteilungen über Forschungsarbeiten auf dem Gebiete des Ingenieurwesens: insbesondere aus den Laboratorien der technischen Hochschulen. 1913, Springer. p. 1-41.

Webb, R. and E. Eckert, Application of rough surfaces to heat exchanger design. international journal of heat and mass transfer, 1972. 15(9): p. 1647-1658